


# Impact of Temporary Link Blockage on Ergodic Capacity of FSO System

Milica I. Petkovic  and Goran T. Djordjevic

**Free-space optical (FSO) systems have attracted much attention from both research and application perspectives owing to their many benefits, such as license-free operation, low-cost, and high data rates. This paper investigates the ergodic capacity of FSO systems, which is an important metric of system performance. The stochastic temporary laser-beam blockage, pointing errors, and atmospheric turbulence are simultaneously considered. The results illustrate that the link blockage causes a decreased ergodic capacity. We show that to maximize the ergodic capacity, there is an optimal value of the laser-beam radius at the waist, which largely depends on pointing errors; however, it is independent of the atmospheric turbulence and the probability of link blockage.**

**Keywords:** Atmospheric turbulence, Ergodic capacity, Free-space optical (FSO) communications, Pointing errors, Temporary link blockage.

## I. Introduction

Optical wireless communication (OWC) has been considered as an alternative or complementary to wireless radio-frequency systems. OWC techniques can be applied to applications including short-distance interconnects on integrated circuits, terrestrial point-to-point links and visible light communications, and satellite-to-ground station links and inter-satellite links. Terrestrial free-space optical (FSO) links support high data rates, require a short time for deployment, and are license free. FSO systems can be applied to provide last-mile access or backhaul connectivity. Moreover, FSO technology is suitable for military applications because the transmission of information is very secure. These systems use wavelengths of 800 nm and 1,550 nm, and they convey information over distances of up to several kilometers [1], [2].

### 1. Literature

As an important metric of the FSO system performance, the channel capacity, which is defined as the maximum data rate that can be transmitted over a channel with an arbitrary small error probability, has been previously analyzed in literature [3]–[13]. When the intensity fluctuations of the received signal are assumed to be very rapid, that is, fading samples at two consequent symbols are independent, the ergodic capacity is a relevant metric. This can be verified by applying an interleaver at the transmitter, and a complementary deinterleaver at the receiver. Some details related to the design of an appropriate interleaver are found in [14]. The expression for the ergodic capacity of an FSO system over a log-normal atmospheric turbulence was derived in [3], while the negative exponential fading statistic was analyzed in

---

Manuscript received July 31, 2017; revised Jan. 3, 2018; accepted Mar. 5, 2018.  
Milica I. Petkovic (corresponding author, milica.petkovic@uns.ac.rs) is with the Faculty of Technical Sciences, University of Novi Sad, Serbia.  
Goran T. Djordjevic (goran@elfak.ni.ac.rs) is with the Faculty of Electronic Engineering, University of Nis, Serbia.

This is an Open Access article distributed under the term of Korea Open Government License (KOGI) Type 4: Source Indiction + Commercial Use Prohibition + Change Prohibition (<http://www.kogil.or.kr/info/licenseTypeEn.do>).

[4]. The capacity performance of the FSO channel under the strong atmospheric turbulence described by the  $K$  distribution is presented in [5], [6]. In [7]–[10], the expression for the ergodic capacity of the FSO channel under the influence of the Gamma-Gamma atmospheric turbulence was derived. In addition to the Gamma-Gamma atmospheric turbulence, the effect of the pointing errors was analyzed in [10] and [11]. In [11], the ergodic capacity was reported in integral form, while Ref. [10] presented corresponding closed-form expressions in terms of Meijer’s  $G$ -functions. In [10], the expression for the ergodic capacity was derived under the assumption that the parameter that describes the misalignment fading, denoted here by  $\zeta$ , is much greater than one. Furthermore, in [12], the ergodic capacity analysis of the FSO link was performed, and considered various atmospheric turbulence models in combination with a nonzero pointing error model. In addition, the ergodic capacity of a mixed radio-frequency/FSO relaying system was observed in [15]–[17].

2. Contribution

In this paper, we derive precise analytical expressions for the ergodic capacity of the FSO link influenced by combined effects of the Gamma-Gamma atmospheric turbulence, pointing errors, and path loss. The novel expression for the ergodic capacity differs from the corresponding result in [10] in the sense that no approximation that is related to the pointing error parameter is introduced here.

In addition, as the main contribution of the paper, the effect of the system failure owing to the stochastic temporary laser beam blockage is considered. The stochastic temporary optical laser beam blockage occurs as a consequence of some random obstacles, such as birds and insects [18]. On the basis of the measured values of the probability of the FSO link blockage presented in [18], the conclusion is that this type of event is not so rare in practice. Derived results are utilized to optimize the beam radius at the waist in order to achieve maximum values of ergodic capacity.

3. Structure

The rest of the paper is organized as follows. Section II describes the system and channel model providing the probability density function (PDF) of the instantaneous signal-to-noise ratio (SNR). Section III presents the ergodic capacity analysis, while the numerical results and discussion are given in Section IV. Some concluding remarks are presented in Section V.

II. PDF of Instantaneous SNR

An FSO that employs intensity modulation/direct detection with on-off keying was considered. The system model is presented in Fig. 1. The information signal is 0 or  $2P_t$ , where  $P_t$  denotes the average transmitted optical power. The received instantaneous SNR is defined as [19, (9)]

$$\gamma = \frac{2P_t^2 \eta^2 h^2}{\sigma_n^2}, \tag{1}$$

with  $\eta$  denoting the optical-to-electrical conversion coefficient,  $h$  is the normalized channel fading coefficient, and  $\sigma_n^2$  is the power of white Gaussian noise. The received signal intensity fluctuations are caused by the Gamma-Gamma atmospheric turbulence, path loss, and pointing errors. The PDF of the received signal intensity,  $h$ , is given by [19, (13)]. Consequently, the PDF of  $\gamma$  is derived as [19, (19)]

$$f_\gamma(\gamma) = \frac{\zeta^2}{2\Gamma(\alpha)\Gamma(\beta)\gamma} G_{1,3}^{3,0} \left( \alpha\beta\kappa\sqrt{\frac{\gamma}{\mu}} \middle| \begin{matrix} \zeta^2 + 1 \\ \zeta^2, \alpha, \beta \end{matrix} \right), \tag{2}$$

where  $G_{p,q}^{m,n}(\cdot)$  denotes the Meijer’s  $G$ -function [20, (07.34.02.0001.01)] and  $\kappa = \zeta^2 / (\zeta^2 + 1)$ . The atmospheric turbulence parameters  $\alpha$  and  $\beta$  are determined as [19, (14)]

$$\alpha = \left( \exp \left[ 0.49\sigma_R^2 / \left( 1 + 1.11\sigma_R^{12/5} \right)^{7/6} \right] - 1 \right)^{-1}, \tag{3}$$

$$\beta = \left( \exp \left[ 0.51\sigma_R^2 / \left( 1 + 0.69\sigma_R^{12/5} \right)^{5/6} \right] - 1 \right)^{-1}.$$

The Rytov variance is denoted as [19, (15)]

$$\sigma_R^2 = 1.23C_n^2 k^{7/6} L^{11/6}, \tag{4}$$

where  $k = 2\pi/\lambda$  is the wave number,  $\lambda$  is the wavelength, and  $L$  is the propagation distance. The refractive index structure parameter,  $C_n^2$ , determines the atmospheric turbulence strength.

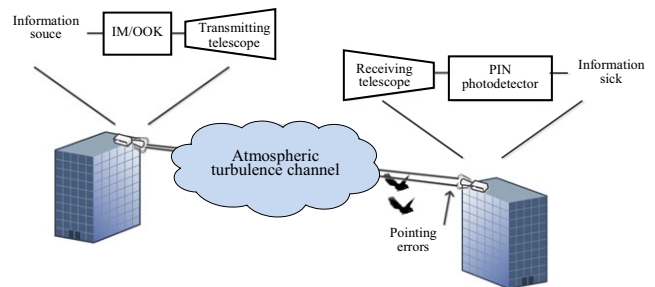


Fig. 1. System model.

The parameter  $\xi$  denotes the ratio between the equivalent beam radius at the receiver,  $z_{Leq}$ , and the jitter standard deviation,  $\sigma_s$ , as  $\xi = z_{Leq}/(2\sigma_s)$ . The equivalent beam radius at the receiver is linked to the beam radius at distance  $L$ ,  $z_L$ , as  $z_{Leq}^2 = z_L^2 \sqrt{\pi} \operatorname{erf}(v)/(2v \exp(-v^2))$ ,  $v = \sqrt{\pi} a/(\sqrt{2} z_L)$ , where  $a$  is the radius of a circular detector aperture and  $\operatorname{erf}(\cdot)$  is the error function [20, (06.25.02.0001.01)]. Parameter  $z_L$  is related to the beam radius at the waist,  $z_0$ , and radius of curvature,  $F_0$ , as  $z_L = z_0 \left( (\Theta_o + \Lambda_o) \left( 1 + 1.63 \sigma_R^{12/5} \Lambda_1 \right) \right)^{1/2}$ , where  $\Theta_o = 1 - L/F_0$ ,  $\Lambda_o = 2L/(kz_0^2)$  and  $\Lambda_1 = \Lambda_o/(\Theta_o^2 + \Lambda_o^2)$  [21].

The average electrical SNR is defined as [19, (18)]

$$\mu = \frac{2P_t \eta^2 \kappa^2 A_0^2 h_l^2}{\sigma_n^2}, \tag{5}$$

with the atmospheric path loss described by the exponential Beers-Lambert law as  $h_l = \exp(-\sigma L)$ , where  $\sigma$  denotes the atmospheric attenuation coefficient for clear air terms. The parameter  $A_0$  is the maximal fraction of the collected power, defined as  $A_0 = [\operatorname{erf}(v)]^2$ , [22].

In addition, optical signal transmission (laser beam) may be interrupted by some kind of moving obstacle coming from the atmospheric surrounding (bird, insect etc.) [18]. If  $p_s$  represents the probability of optical signal blockage, the PDF of the instantaneous SNR,  $\gamma$ , is defined as

$$f_N(\gamma) = p_s \delta(\gamma) + (1 - p_s) f_\gamma(\gamma), \tag{6}$$

where  $\delta(\cdot)$  is the Dirac delta function [20, (14.03.02.0001.01)].

### III. Ergodic Capacity Analysis

If the duration of a symbol is greater than the time over which the channel is significantly correlated, the ergodic capacity is an appropriate measure for FSO system performance, which is defined as [7], [9], [10]

$$C = B \int_0^\infty \log_2(1 + \gamma) f_N(\gamma) d\gamma, \tag{7}$$

where  $B$  is the channel bandwidth. By substituting (6) into (7), after applying [20, (14.03.21.0003.01)] as

$$B p_s \int_0^\infty \log_2(1 + \gamma) \delta(\gamma) d\gamma = B p_s \log_2(1 + 0) = 0, \tag{8}$$

and [20, (01.05.26.0002.01)] to represent the logarithm function in terms of Meijer's  $G$ -function as

$$\log_2(1 + \gamma) = \frac{1}{\ln(2)} G_{2,2}^{1,2} \left( \gamma \left| \begin{matrix} 1, & 1 \\ 1, & 0 \end{matrix} \right. \right), \tag{9}$$

the ergodic capacity in (7) is re-written as

$$C = B \frac{(1 - p_s) \xi^2}{2 \ln(2) \Gamma(\alpha) \Gamma(\beta)} \int_0^\infty \gamma^{-1} G_{2,2}^{1,2} \left( \gamma \left| \begin{matrix} 1, & 1 \\ 1, & 0 \end{matrix} \right. \right) \times G_{1,3}^{3,0} \left( \alpha \beta \kappa \sqrt{\frac{\gamma}{\mu}} \left| \begin{matrix} \xi^2 + 1 \\ \xi^2, & \alpha, & \beta \end{matrix} \right. \right) d\gamma. \tag{10}$$

The integral in (10) is solved using a rule for integrating the product of two Meijer's  $G$ -functions given in [20, (07.34.21.0013.01)]. The Meijer's  $G$ -function in the obtained expression can be transformed by employing permutations of the parameters using [20, (07.34.04.0003.01), and (07.34.04.0004.01)]. Afterwards, it is simplified by [20, (07.34.03.0002.01)]. The ergodic channel capacity has the final form as

$$C = B \frac{(1 - p_s) 2^{\alpha+\beta-3} \xi^2}{\pi \ln(2) \Gamma(\alpha) \Gamma(\beta)} \times G_{3,7}^{7,1} \left( \frac{\alpha^2 \beta^2 \kappa^2}{16\mu} \left| \begin{matrix} 0, & 1, & \frac{\xi^2+2}{2} \\ & & \chi_1 \end{matrix} \right. \right), \tag{11}$$

where  $\chi_1 = \frac{\xi^2}{2}, \frac{\alpha}{2}, \frac{\alpha+1}{2}, \frac{\beta}{2}, \frac{\beta+1}{2}, 0, 0$ . Note that  $p_s = 0$  leads to the case when there is no blockage, and the FSO signal transmission will be certainly performed. Otherwise,  $p_s = 1$  represents the case when the signal will be definitely blocked, and the transmission will be interrupted. Assuming  $p_s = 0$ , (11) is an alternative form of the result given in [10, (22)]. Note that the assumption of  $\xi^2 \gg 1$  is not utilized as in [10]. A comparison of numerical results that were obtained based on (11) and [10, (22)] will be presented in the next section.

When pointing errors are negligible, the ergodic capacity can be derived by taking the limit of (11) for  $\xi^2 \rightarrow \infty$ . After applying [20, (07.34.25.0007.01), (07.34.25.0006.01) and (06.05.16.0002.01)], the ergodic capacity of the FSO link when intensity fluctuations are caused only by the Gamma-Gamma atmospheric turbulence is derived as

$$C_{GG} = B \frac{(1 - p_s) 2^{\alpha+\beta-2}}{\pi \ln(2) \Gamma(\alpha) \Gamma(\beta)} \times G_{2,6}^{6,1} \left( \frac{\alpha^2 \beta^2}{16\mu} \left| \begin{matrix} 0, & 1 \\ \frac{\alpha}{2}, & \frac{\alpha+1}{2}, & \frac{\beta}{2}, & \frac{\beta+1}{2}, & 0, & 0 \end{matrix} \right. \right). \tag{12}$$

If there is no signal blockage ( $p_s = 0$ ), after using [20, (07.34.16.0001.01)], the convenient alternation is done; therefore, (12) is reduced to the results reported in [7,

(16)], [8, (21)], [9, (10)] [10, (11)]. When parameter  $\beta = 1$ , the Gamma-Gamma model reduces to the  $K$  distribution. Applying [20, (07.34.16.0001.01)] and assuming  $\beta = 1$  and  $p_s = 0$ , (12) comes to [5, (8)].

#### IV. Numerical Results

This section presents numerical results, which are obtained by using the analytical expression in (11) derived in the previous section. The presented novel analytical expressions for the ergodic channel capacity, which are derived in terms of the Meijer's  $G$ -function, can be numerically evaluated using well-known software packages such as Mathematica, Matlab, or Maple. In addition, Monte Carlo simulations are presented to confirm analytical expressions. Monte Carlo simulations are performed in Matlab on the basis of  $10^9$  generated samples as follows.

The received signal intensity sample is determined as a product of factors related to the atmospheric turbulence, pointing errors, and path loss, such as,  $h = h_a h_p h_l$ . The sample  $h_a$  represents the random variable related to Gamma-Gamma atmospheric turbulence, which is obtained as  $h_a = h_{aX} \times h_{aY}$ , where  $h_{aX}$  and  $h_{aY}$  are mutually independent Gamma random variables modeled by a Gamma distribution. Based on algorithms from [23], [24], random variables  $h_{aX}$ , and  $h_{aY}$  are generated. The path-loss component  $h_l$  is deterministic, and it is calculated based on [19, (12)], [22]. The misalignment fading sample  $h_p$ , which is related to pointing errors, is generated based on [22, (9)]. Based on the aforementioned results, the signal intensity sample  $h$  can be generated; thus, the SNR sample is generated in a straightforward manner by considering (1) and (6). In our work, the values of  $p_s$  are chosen as examples in order to perform the analysis, while some experimental measurements are presented in [18]. In the subsequent analysis, it can be observed that the numerical results are in agreement with the simulation results.

Atmospheric turbulence strength is determined by the refractive index structure parameter as follows:  $C_n^2 = 6 \times 10^{-15} \text{ m}^{-2/3}$  for weak atmospheric turbulence conditions,  $C_n^2 = 2 \times 10^{-14} \text{ m}^{-2/3}$  for moderate atmospheric turbulence conditions, and  $C_n^2 = 5 \times 10^{-14} \text{ m}^{-2/3}$  for strong atmospheric turbulence conditions [19]. The atmospheric attenuation coefficient  $\sigma$  takes a value  $\sigma = 0.44 \text{ dB/km}$ , which corresponds to clear-air terms. The wavelength  $\lambda = 1,550 \text{ nm}$ , noise standard deviation  $\sigma_n = 10^{-7} \text{ A/Hz}$ , and optical-to-electrical conversion coefficient  $\eta = 0.8$  are considered. The radius of a circular detector aperture takes a value  $a = 5 \text{ cm}$ , while the radius of curvature is  $F_0 = -10 \text{ m}$  [19], [21].

Figure 2 presents the dependence of the ergodic capacity on the probability of signal blockage for different values of normalized jitter standard deviation under various atmospheric turbulence conditions. The largest-capacity value exists for  $p_s \rightarrow 0$ , and corresponds to the case when there is no signal blockage. As the value of  $p_s$  increases, the ergodic capacity performance worsens. When  $p_s = 1$ , the laser beam is clearly blocked by some kind of obstacle, which leads to system failure. Under all turbulence conditions and for all values of the normalized jitter standard deviation, the ergodic capacity is relatively constant within the range of blockage probabilities less than  $10^{-2}$ , while the ergodic capacity sharply decreases for blockage probability values greater than  $10^{-1}$ . When the probability of signal blockage is very high,  $p_s > 0.7$ , and the influence of pointing errors and atmospheric turbulence impairments has less of an impact on system performance.

The dependence of the ergodic capacity on the beam radius at the waist for different values of the normalized jitter standard deviation under various turbulence conditions is presented in Fig. 3. The case when there is no signal blockage is considered ( $p_s = 0$ ), as well as the case when the probability of signal blockage is  $p_s = 0.2$ . The maximum ergodic capacity corresponds to a specific optimal value of  $z_0$ . Hence, the proper selection of the transmitter aperture significantly impacts improvements in the system performance. It should be noted that the value of  $z_{0\text{opt}}$  is highly dependent on the normalized jitter standard deviation, while the atmospheric turbulence conditions are of less importance to the value of  $z_{0\text{opt}}$ . In addition, Fig. 4 shows the ergodic capacity dependence on the beam radius at the waist for different values of  $p_s$ . It

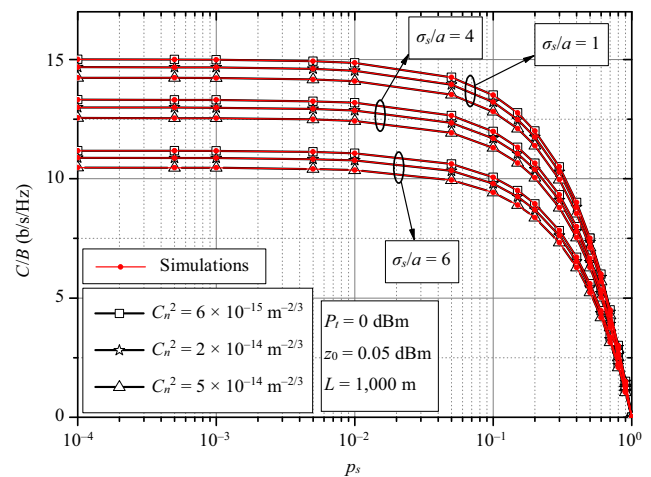


Fig. 2. Normalized ergodic capacity versus probability of blockage.

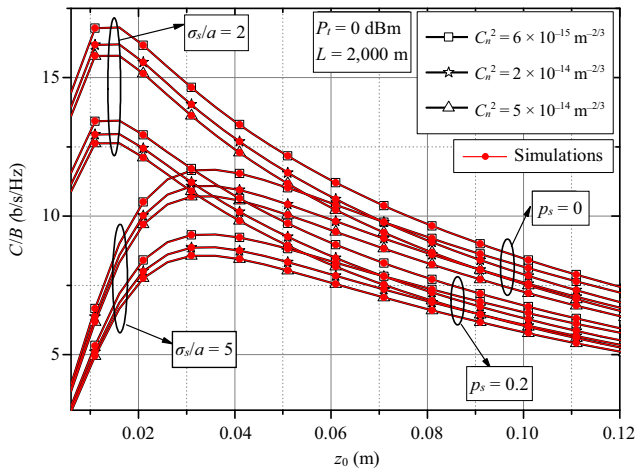


Fig. 3. Normalized ergodic capacity versus beam radius at the waist.

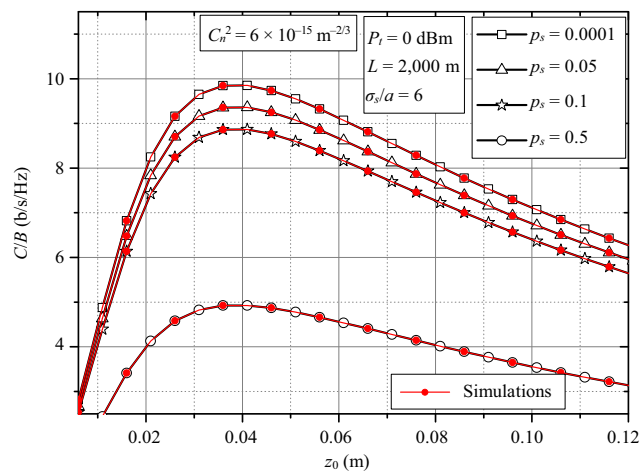


Fig. 4. Normalized ergodic capacity versus beam radius at the waist for different values of probability of signal blockage.

can be concluded that the probability of signal blockage does not influence the optimal value of the beam radius at the waist. In other words, the maximum ergodic capacity is independent of the probability that the signal can be blocked by some kind of obstacle.

Table 1 presents the estimated values of  $z_{0opt}$  for different values of the normalized jitter standard deviation and average transmitted optical power in various

Table 1. Optimum values of the beam radius at the waist  $z_{0opt}$  (cm).

$P_t$ (dBm)	$\sigma_s/a = 2$			$\sigma_s/a = 5$		
	Weak	Moderate	Strong	Weak	Moderate	Strong
-10	1.28	1.27	1.25	2.96	2.91	2.89
10	1.34	1.34	1.34	3.49	3.48	3.47

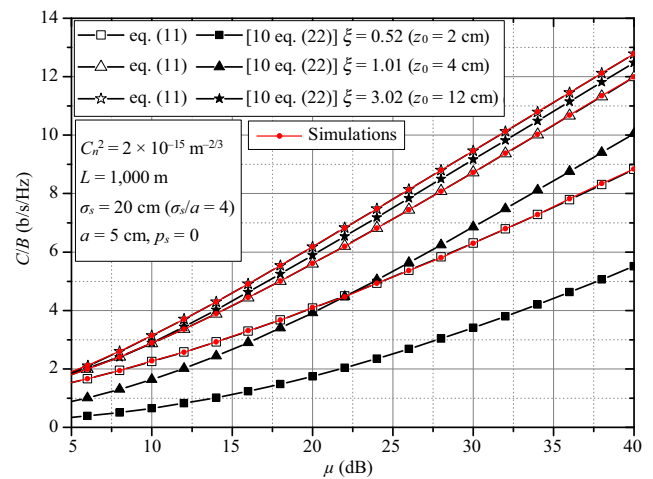


Fig. 5. Normalized ergodic capacity for various degrees of misalignment.

atmospheric turbulence conditions. As already noted, the normalized jitter standard deviation significantly impacts the proper choice of  $z_{0opt}$ . As the values of  $\sigma_s/a$  increase, the value of  $z_{0opt}$  increases. Next, lower values of the average transmitted optical power result in smaller values of the beam radius at the waist in order to achieve maximum of ergodic capacity. In addition, poor atmospheric conditions correspond to lower values of  $z_{0opt}$ .

Figure 5 presents numerical results based on (11) together with those obtained using [10, (22)]. It is evident that there is a disagreement between the numerical values of the ergodic capacity that are estimated using these two equations. For example, for  $\mu = 30$  dB, estimated values of the ergodic capacity corresponding to [10, (22)] and (11) are 3.4 b/s/Hz and 6.3 b/s/Hz, respectively. This disagreement appears to be because [10, (22)] was derived under the assumption of  $\zeta \gg 1$ , which was noted in [10]. As expected, the disagreement between numerical values of the ergodic capacity decreases with increasing values of  $\zeta$ . A comparison with Monte Carlo simulation shows that the accuracy of (11) is very good, and can be used even for low values of parameter  $\zeta$ .

## V. Conclusions

The main aim of the paper is to investigate the ergodic capacity performance of the FSO system when the stochastic temporary blockage of the laser beam is considered, which occurs as a result of some moving obstacles in atmospheric environments. It has been concluded that the optical beam blockage can lead to significant ergodic capacity performance degradations. In

addition, the maximization of the ergodic capacity can be achieved by proper selection of the FSO transmitting aperture. It has been noted that the optimal value of the laser beam radius at the waist is highly dependent on the jitter standard deviation. However, the probability of optical beam blockage and atmospheric turbulence conditions have a negligible impact on the optimal value of the laser beam radius at the waist, while a greater average transmitted optical power leads to a larger value of  $z_{0\text{opt}}$ .

## Acknowledgements

This work was supported by the Ministry of Education, Science and Technology Development of the Republic of Serbia (TR-32035 – “Development of dialogue systems for Serbian and other South Slavic languages,” TR-32028 – “Advanced techniques for efficient use of spectrum in wireless systems” and III 44006 – “Development of new information and communication technologies, based on advanced mathematical methods, with applications in medicine, telecommunications, power systems, protection of national heritage and education”).

## References

- [1] Z. Ghassemlooy, W. Popoola, and S. Rajbhandari, *Optical Wireless Communications: System and Channel Modelling with MATLAB®*, Boca Raton, FL, USA; CRC Press, Taylor & Francis Group, 2012.
- [2] M.A. Khalighi and M. Uysal, “Survey on Free Space Optical Communication: A Communication Theory Perspective,” *IEEE Commun. Surveys Tut.*, vol. 16, no. 4, 2014, pp. 2231–2258.
- [3] H.E. Nistazakis, G.S. Tombras, A.D. Tsigopoulos, E.A. Karagianni, and M.E. Fafalios, “Average and Outage Capacity Estimation of Optical Wireless Communication Systems Over Weak Turbulence Channels,” in *Proc. Mosharaka Int. Conf. Commun., Propag., Electron.*, Amman, Jordan, Jan. 2009.
- [4] H.E. Nistazakis, V.D. Assimakopoulos, and G.S. Tombras, “Performance Estimation of Free Space Optical Links Over Negative Exponential Atmospheric Turbulence Channels,” *Optik-Int. J. Light Electron Opt.*, vol. 122, no. 24, Dec. 2011, pp. 2191–2194.
- [5] H.G. Sandalidis and T.A. Tsiftsis, “Outage Probability and Ergodic Capacity of Free-Space Optical Links Over Strong Turbulence,” *Electron. Lett.*, vol. 44, no. 1, Jan. 2008, pp. 46–47.
- [6] H.E. Nistazakis et al., “Estimation of Capacity Bounds of Free Space Optical Channels Under Strong Turbulence Conditions,” in *Proc. Int. Conf. Microw. Radar Wireless Commun.*, Vilnius, Lithuania, June 14–16, 2010, pp. 1–3.
- [7] H.E. Nistazakis, E.A. Karagianni, A.D. Tsigopoulos, M.E. Fafalios, and G.S. Tombras, “Average Capacity of Optical Wireless Communication Systems Over Atmospheric Turbulence Channels,” *J. Lightw. Technol.*, vol. 27, no. 8, Apr. 2009, pp. 974–979.
- [8] H.E. Nistazakis, T.A. Tsiftsis, and G.S. Tombras, “Performance Analysis of Free-Space Optical Communication Systems Over Atmospheric Turbulence Channels,” *IET Commun.*, vol. 3, no. 8, Aug. 2009, pp. 1402–1409.
- [9] H.E. Nistazakis, G.S. Tombras, A.D. Tsigopoulos, E.A. Karagianni, and M.E. Fafalios, “Capacity Estimation of Optical Wireless Communication Systems Over Moderate to Strong Turbulence Channels,” *J. Commun. Netw.*, vol. 11, no. 4, Aug. 2009, pp. 384–389.
- [10] W. Gappmair, “Further Results on the Capacity of Free-Space Optical Channels in Turbulent Atmosphere,” *IET Commun.*, vol. 5, no. 9, 2011, pp. 1262–1267.
- [11] I.E. Lee, Z. Ghassemlooy, W.P. Ng, and M. Uysal, “Performance Analysis of Free Space Optical Links Over Turbulence and Misalignment Induced Fading Channels,” in *Proc. Int. Symp. Commun. Syst., Netw. Digital Signal Proc.*, Poznan, Poland, July 2012, pp. 1–6.
- [12] I.S. Ansari, M.-S. Alouini, and J. Cheng, “Ergodic Capacity Analysis of Free-Space Optical Links With Nonzero Boresight Pointing Errors,” *IEEE Trans. Wireless Commun.*, vol. 14, Aug. 2015, pp. 4248–4264.
- [13] A. Lapidath, S.M. Moser, and M.A. Wigger, “On the Capacity of Free-Space Optical Intensity Channels,” *IEEE Trans. Inform. Theory*, vol. 55, no. 10, Oct. 2009, pp. 4449–4461.
- [14] F.M. Davidson and Y.T. Koh, “Interleaved Convolutional Coding for the Turbulent Atmospheric Optical Communication Channel,” *IEEE Trans. Commun.*, vol. 36, Sept. 1988, pp. 993–1003.
- [15] B. Bag, A. Das, A. Chandra, and C. Bose, “Capacity Analysis for Rayleigh/Gamma-Gamma Mixed RF/FSO Link with Fixed-Gain AF Relay,” *IEICE Trans. Commun.*, vol. 100, no. 10, 2017, pp. 1747–1757.
- [16] I.S. Ansari, F. Yilmaz, and M.S. Alouini, “Impact of Pointing Errors on the Performance of Mixed RF/FSO Dual-Hop Transmission Systems,” *IEEE Wireless Commun. Lett.*, vol. 2, no. 3, 2013, pp. 351–354.
- [17] J. Vellakudiyani, I.S. Ansari, V. Palliyembil, P. Muthuchidambaramanathan, and K.A. Qaraqe, “Channel Capacity Analysis of a Mixed Dual-Hop Radio-Frequency–Free Space Optical Transmission System With Málaga Distribution,” *IET Commun.*, vol. 10, no. 16, 2016, pp. 2119–2124.

- [18] Z. Kolka, O. Wilfert, D. Biolek, and V. Biolkova, "Availability Model of Free-Space Optical Data Link," *Int. J. Microw. Opt. Technol.*, vol. 1, no. 1, Aug. 2006, pp. 612–616.
- [19] G.T. Djordjevic, M. Petkovic, A. Cvetkovic, and G.K. Karagiannidis, "Mixed RF/FSO Relaying With Outdated Channel State Information," *IEEE J. Sel. Areas Commun.*, vol. 33, no. 9, Sept. 2015, pp. 1935–1948.
- [20] The Wolfram Functions Site, 2008, Accessed, 2017. <http://functions.wolfram.com>
- [21] A.A. Farid and S. Hranilovic, "Outage Capacity for MISO Intensity Modulated Free-Space Optical Links With Misalignment," *IEEE/OSA J. Opt. Commun. Netw.*, vol. 3, no. 10, Oct. 2011, pp. 780–789.
- [22] A.A. Farid and S. Hranilovic, "Outage Capacity Optimization for Free Space Optical Links with Pointing Errors," *J. Lightw. Technol.*, vol. 25, no. 7, 2007, pp. 1702–1710.
- [23] G. Marsaglia and W.W. Tsang, "A Simple Method for Generating Gamma Variables," *ACM Trans. Math. Softw.*, vol. 26, no. 3, Jan. 2000, pp. 363–372.
- [24] D. Kundu and R.D. Gupta, "A Convenient Way of Generating Gamma Random Variables Using Generalized Exponential Distribution," *Comput. Stat. Data Anal.*, vol. 51, no. 6, Mar. 2007, pp. 2796–2802.



**Milica I. Petkovic** received her MS and PhD degrees in electrical engineering from the Faculty of Electronic Engineering, University of Nis, Serbia, in 2010 and 2016, respectively. Her PhD degree was in the field of free-space optical systems. She worked as a research assistant with the

Department of Telecommunication within the Faculty of Electronic Engineering, University of Nis, Serbia. Currently, she is with the Department of Power, Electronics, and Telecommunication Engineering, Faculty of Technical Sciences, University of Novi Sad, Serbia. Her main research interests include communication theory as well as wireless and optical communication systems.



**Goran T. Djordjevic** received his BS, MS, and PhD degrees in electrical engineering from the University of Nis, Faculty of Electronic Engineering, Serbia, in 1996, 1999, and 2005, respectively. He is a full professor at the Department of Telecommunications, Faculty of Electronic

Engineering, University of Nis, Serbia. He teaches courses in Communication Theory, Modeling and Simulation of Communication Systems, and Information Theory and Satellite Communications. His area of interest is communication theory and satellite applications, as well as wireless and optical communication systems. His current research interests include the application of different modulation formats and error-correction codes in free-space optical systems, as well as the modeling and simulation of fading channels and synchronization problems. He has published more than 40 high-ranked journal papers and more than 150 conference papers. He is also an author of two textbooks (in Serbian) in communication theory. He has participated in several FP7, C.O.S.T. and TEMPUS projects supported by the EU, one project supported by the Ministry of Foreign Affairs of Norway, and several projects in the field of communications supported by Ministry of Education, Science, and Technological Development of the Republic of Serbia.